JOURNAL OF MATERIALS SCIENCE **39** (2004) 1927– 1933

Electroless metal plating of microtubules: Effect of microtubule-associated proteins

YI YANG*,‡
Department of Materials Science and Engineering, The University of Arizona, Tucson, AZ 85721, USA

B. H. CONSTANCE
Department of Chemical and Environmental Engineering, The University of Arizona, Tucson, AZ 85721, USA

P. A. DEYMIER
Department of Materials Science and Engineering, The University of Arizona, Tucson, AZ 85721, USA
E-mail: deymier@u.arizona.edu

J. HOYING
Biomedical Engineering Program GIDP, The University of Arizona, Tucson, AZ 85724, USA

S. RAGHAVAN, B. J. J. ZELINSKI
Department of Materials Science and Engineering, The University of Arizona, Tucson, AZ 85721, USA

Microtubules (MTs) are self-assembled proteinaceous filaments with nanometer scale diameters and micrometer scale lengths. Their aspect ratio, the reversibility of their assembly and their ability to be metallized by electroless plating make them good candidates to serve as templates for the fabrication of nanowires. We have shown that microtubule-associated-proteins (MAPs) play a critical role in maintaining the MT stability during Pt-catalyzed electroless Ni plating. MAP-stabilized MTs metallized for one minute in a Ni-acetate-based electroless-plating bath are coated with a metal film only several nanometers thick. The MAPs appear to lead to the formation of nanometer-wide metal bridges between the MTs. The metal coatings are constituted of small Pt clusters (∼3 nm), distributed and oriented randomly, embedded in an amorphous nickel matrix.

1. Introduction

In recent years, the exponential growth in semi conductor technology has been sustained by extending the capabilities of top-down manufacturing processes based on lithography to shorter and shorter wavelengths. Unfortunately, the costs of these top-down approaches are projected to be prohibitive at sizes and tolerances in the nanometer size range. In response, a new paradigm has arisen based on the bottom-up or molecular engineering approach to the mass replication of nano-scale electronic circuits that promises to be cheaper, more flexible, and efficient. Control of interconnections emerges as one of the major challenges in the development of these bottom-up approaches. The construction of functional nano-scale electronic devices using a bottom-up approach requires self-assembly processes [1].

Several routes involving self-assembly of organic materials have already been followed. Techniques based on self-assembly of DNA-functionalized nanoparticles have been reported [2, 3]. The use of absorbed organic molecules and DNA for self-assemble nanoscale metal rods made by electrochemical replication of porous membranes has been reported [4]. Others have coated DNA strands with metal, thus forming a conductive wire between two-electrodes [5]. Other studies have used polypeptides and/or proteins as templates for nanowires. Several surfactant-like peptides have been shown to undergo self-assembly forming nanotubes with a variety of diameters [6]. Peptide nanotubules can also be coated with proteins such as avidin enabling the use of biological interactions based on molecular recognition [7]. Avidin-coated peptide tubules have been anchored as bridges onto biotin-incorporated self-assembled monolayers on Au substrates [8]. Alternatively, metallization of proteinaceous nanotubules derived from bacteria's rhapidosomes

*Author to whom all correspondence should be addressed.
‡*Present address*: Department of Materials Science and Engineering, University of Arizona, Tucson, AZ 85719, USA.

have been produced [9]. Proteins that self-assemble into long fibers, such as yeast prion proteins and tubulin, provide biological interactions with a naturally high specificity and can serve directly as templates for metal nanowires [10, 11].

In this paper, we focus on MTs as templates for fabricating metallic nanowires. MTs are self-assembling, dynamic, and tubular shaped biomolecules with diameters of approximately 24 nm and large aspect ratios, made from polymerized tubulin proteins. MTs exhibit dynamic instability at some critical tubulin concentration during which they apparently undergo random successive periods of assembly and disassembly. Additionally, the stability of MTs is very sensitive to the chemical environment and temperature. Several proteins, called microtubule-associated proteins (MAPs) have MT-binding activity and play important roles in MT polymerization and regulation, including the stabilization of polymerized MTs [12]. Because of repeatable residues of the surface of MTs, people also can use them as bioorganic templates for structurally defined nanoparticle arrays [13].

Metallization of MTs has been demonstrated by surface activation with palladium followed by electroless plating of nickel [14]. During electroless plating, it appears that Ni is essentially deposited on the external surface of the microtubule [11]. It was also shown that MT metallization required pH and temperature conditions approaching those for *in-vitro* MT assembly. It is not known if MT can survive other conditions more conducive to a variety of electroless plating methods.

In our work, we have investigated the electroless plating of pure and MAP-rich MTs in further detail. Following the activation of the MT surface with Pt, electroless plating is used to deposit Ni on the Pt-activated MT surfaces. We have paid particular attention to the role of MAPs in the stabilization of the MT templates during all the steps of metallization. Field Emission Scanning Electron Microscopy (FESEM), Transmission Electron Microscopy (TEM) and High-resolution Electron Microscopy (HREM) are used to provide a detailed characterization of the morphology, structure and composition of the metallized, MAP-stabilized, microtubules. Results concerning the stability of pure MTs and MAP-rich MTs in the activating Pt solution are presented and discussed. We detail the morphological, microstructural and compositional characterization of MAP-stabilized Ni-plated MTs. Finally, some conclusions are drawn concerning the role of MAPs in the fabrication of metal nanowires using electroless plating of MTs templates.

2. Materials and methods

In order to study the effect of MAPs on the stability of MTs in electroless plating solutions, we used both high purity tubulin proteins (>99% tubulin monomer) and low purity MAP-rich tubulin (∼30% MAPs). Both tubulin preparations were prepared from bovine brain extracts (Cytoskeleton Inc), and were stored at −70°C in G-PEM buffer (pH 6.8). The buffer contained 80 mM Piperazine-N, N′-bis(2-ethanesulfonic acid) sequisodium salt (PIPES), 1 mM Magnesium chloride ($MgCl_2$); 1 mM Ethylene glcol-bis(b-amino-ethyl ether) N,N,N′,N′-tetra-acetic acid (EGTA) and 1 mM Guanosine 5′-triphosphate (GTP).

In-vitro MT assembly was performed in PEM 80 buffer (80 mM PIPES, 1 mM EGTA, 4 mM $MgCl_2$, using KOH to adjust PH to 6.9) with a final concentration of tubulin of 1.5 mg/ml. Polymerization was performed by the addition of GTP (final concentration is 0.25 mM) and taxol (final concentration is 10 μM) was either included in the reaction or added after polymerization takes place (see later). Researches [17, 18] show that Taxol can stabilize microtubules both during and after the polymerization. So, two approaches were taken in polymerizing MTs. The first approach involved polymerization of MTs in the presence of taxol. In the second approach, taxol (∼20 μM) was added as a stabilizing agent after polymerization of the MTs was completed. During both approaches, the solutions were rotated at low speed (15 rpm) for 30 min at 37°C for polymerization. Then, the solution was centrifuged at 14500 g for 30 min to separate MTs from the unpolymerized tubulin. The supernatant was removed and about 5-fold volume of fresh PEM 80 buffer was added to resuspend the MTs.

The stability of pure MTs and MAP_rich MTs were tested in electroless plating solution developed by Kirsch *et al*. [14]. MTs were metallized in a two-step procedure. In the first step, the MT surface was activated with 3 mM K_2PtCl_4 (pH = 6.2). This Pt(II) solution was prepared and stored at room temperature for at least one day before use. Equal volumes of Pt solution plus prepared MTs solution were mixed and kept in the dark for 2 h for surface activation. The catalyzed MTs were washed two times using PEM 80 buffer by ultra filtration with a 300 k-Da MW cutoff membrane filter. The pellet thus obtained was dispersed in an equal amount of PEM 80 buffer and mixed with an equal amount of metallization bath containing nickel Acetate (50 g/l), sodium citrate (25 g/l), lactic acid 85% (25 g/l), and a reducing agent–DMAB (Borane-dimethylamine complex, 2.5 g/l), during which, DMAB functions as a reducing agent. NH_4OH (1.0 M) was added to adjust the pH to 6.9. The reaction was stopped by diluting the solution 100-fold with double distilled H_2O.

Optical characterization of pure MTs, MAP-stabilized MTs and Pt-activated MTs was conducted with an epi-fluorescence microscope. MTs were visualized by fluorescence immuno-labeling using a monoclonal antibody directed against β tubulin as the primary antibody (anti-β-tubulin, clone TUB 2.1, Sigma Inc.) Prepared MTs were incubated with the primary antibody for 30 min at room temperature. A secondary goat antibody, conjugated with Cy3 and directed against mouse IgG (Sigma Inc.) was mixed with the primary antibody-labeled MT for 30 min. Between and after these stages, PBS buffer (Phosphate-buffered saline, pH 7.4) was used for washing. The suspension was then deposited on a poly L-lysine coated microscope glass slide.

Field Emission Scanning electron microscopy (FESEM) was carried out using a Hitachi S-4500 with

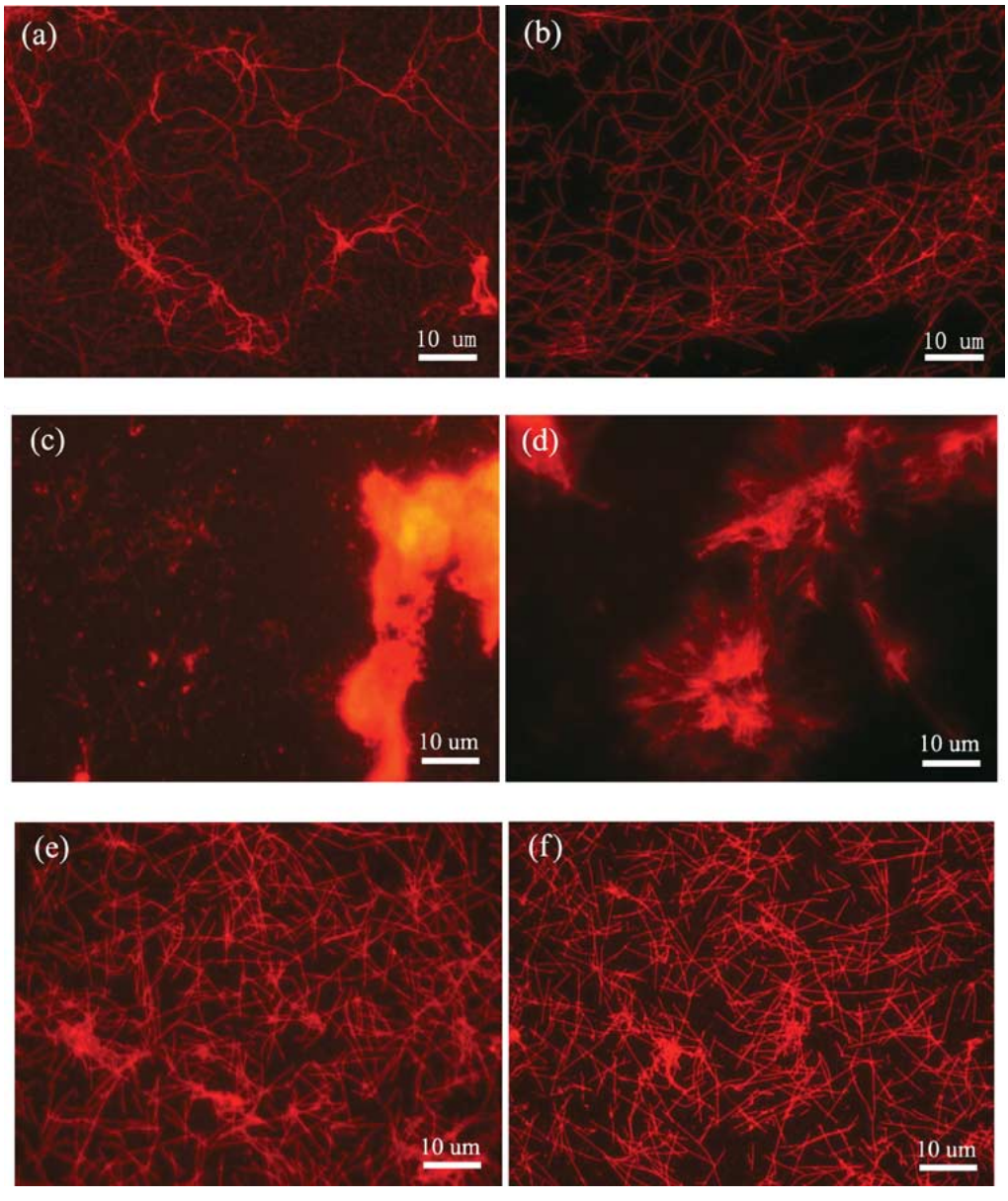

Figure 1 Stability of MTs before and after treating with Pt(II) solution taken by fluorescence microscope (a. MTs grown from pure tubulin with taxol stabilization during growth; b. MTs grown from pure tubulin with taxol stabilization after growth; c. Taxol-stabilized pure MTs after treating with the Pt(II) solution-1; d. Taxol-stabilized pure MTs after treating with the Pt(II) solution-2; e. MAP-stabilized MTs with taxol stabilization during growth; f. MAP-stabilized MTs after treating with the Pt(II) solution).

1.5 nm resolution at 5 kV and equipped with energy dispersive spectroscopy (EDS) capabilities. Transmission electron microscopy (TEM) and high-resolution electron microscopy images were obtained using a Hitachi H8100 equipped with small probe forming lenses for nanodiffraction, operated at 200 kV. MTs samples for SEM and TEM were prepared by pipetting metallized MTs from a suspension onto a carbon coated copper grid followed by drying in a vacuum system.

3. Stability of MTs in Pt(II) activating solution

MTs are assembled from heterodimers formed from two related protein monomers: α and β tubulins. In the proper chemical environment, the tubulin monomers form a heterodimer and self-assemble into the microtubule structure. Tubulin polymerization is facilitated by the addition of guanosine triphosphate (GTP), which is incorporated into the exposed β tubulin of the protofilament and facilitates binding to the adjacent heterodimer by undergoing hydrolysis to guanosine diphosphate (GDP). Self-assembly into the MT begins with nucleation involving tubulin monomers followed by the geometry of self-assembly. Thus a polarized MT containing minus and plus ends is formed by this process. The minus end contains an exposed α tubulin monomer and undergoes slower addition rate than the plus end. In the absence of stabilizing agents, microtubules exist in a dynamic state with net addition of monomers to the plus end and net removal of monomers from the minus end [15]. The dynamic instability of growth and shrinkage *in vitro* occurs at tubulin concentrations near the critical concentration of pure tubulin, which is about 0.088 mg/ml [16]. In our experiments, the concentration of pure tubulin (1.5 mg/ml) is much higher than the critical concentration, and steady state assembly of microtubules is achieved.

Taxol, an anti-cancer drug, can stabilize microtubules. Researches [17, 18] show taxol binds to a pocket in β-tubulin on the microtubule's inner face,

which strongly reduces the ability of the tubulin to dissociate when it becomes exposed at the microtubule end. When taxol is present during polymerization, a high number of MTs can be obtained with lengths of approximately-20 micrometers in average (Fig. 1a). However, MT length is increased approximately 25% when taxol is added only after polymerization is complete (Fig. 1b).

Although taxol-treated MTs polymerized from purified tubulin monomers (with taxol present during or after polymerization) are very stable under normal *in vitro* conditions, they do not withstand the harsh environment present during catalysis and electroless plating. When treated with the catalyzing Pt(II) solution for 2 h, taxol-stabilized (either during or post polymerization), pure MTs disassembled into very small segments and formed some big chunks (Fig. 1c), or formed star-shaped clusters (Fig. 1d).

Microtubule-associated proteins (MAPs) can also stabilize MTs. One major family of MAPs, called assembly MAPs, is responsible for cross-linking microtubules in the cytosol and determines the spacing between individual microtubules. Assembly MAPs bind to the side of microtubules and project outward. When MAPs coat the outer wall of a microtubule, tubulin subunits are unable to dissociate from the polymer. These assembly MAPs can be grouped into two types. Type I MAPs contain several repeats of the amino acid sequence Lys-Lys-Glu-X. Type II MAPs, such as Tau and MAP4, have three or four repeats of an 18-residue sequence in the MT binding domain, which can form fibrous cross-bridges between MTs and also link MTs to intermediate filaments. They also can suppress MT dynamics at very low molar stoichiometric levels relative to tubulin [19] and even affect MT rigidity [20]. In the presence of MAPs and taxol, microtubules can polymerize at temperatures below 37°C [21]. It is evident from Fig. 1f that MAP-stabilized MTs can exist after a two-hour catalysis treatment with the Pt(II) solution. Only a small part of the MTs did not survive the process (compare Fig. 1e to f). Except for a few longer ones, most of the MAP-stabilized MTs have lengths of approximately 10 to 15 micrometers, shorter than the original stock solution of pure MTs (Fig. 1a and b). Brighter filaments are indications of bundled MTs (Fig. 1e and f).

4. Electroless plating and characterization of metallized MTs

The generally made assumption is that Pt(II) or Pt(IV) complexes adsorbed on the surface of MTs first react with the reducing agent (DMAB) to create Pt(0) atoms and form Pt clusters [22]. Due to the specific properties of MTs, there could be one more step in the process of electroless plating. During the stage of treating MTs with Pt(II) aqueous solution, Pt(II) can be attached onto the surface of MTs, via exposed amino acid residues, such as cysteine, histidine and trytophane. These amino acids with weak reducing ability could adsorb Pt(II) and reduce it to an oxidation state higher than zero. Those ions in oxidation states higher than zero and Pt(II) ions are reduced to isolated Pt(0) atoms when exposed to DMAB. After a while, when a critical concentration of Pt(0) atoms is reached, they would aggregate to form metal clusters [23].

These clusters serve as catalytic surfaces and initial nucleation centers for the deposition of the first layer of nickel onto the MTs surface. Nickel will not grow on a surface without metallic Pt cluster. Thus a continuous metal coating of Ni is formed. Then, this newly formed layer functions as a new substrate and nucleation center for further Ni deposition. Thus, the formation and distribution of Pt clusters is a key for the deposition of metals. To maintain a constant deposition rate, we control tightly the pH value at 6.9 and temperature at 37°C. Nickel and reducing agent concentrations were kept at optimum levels.

For pure MTs stabilized with taxol during growth or after growth, one minute after the metallization bath was added, some metal particles visible to the eye precipitated. In contrast electroless plating of MAP-stabilized MTs proceeds in a drastically different manner. After one minute, the solution was only slightly cloudy, without any particles visible to the eye. SEM analysis of metallized pure MTs indicates that there are a few rare, small segments of metal-coated MTs, which are about 100 nanometers in length and about 50 to 60 nanometers in diameter. Some big particles of metal are also found. Considering the template is only 24 nm in diameter, the thickness of the metal film is about 25 to 35 nanometers. We believe that the big particles

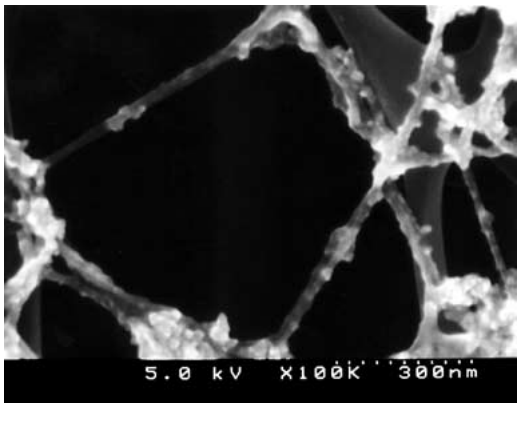

Figure 2 SEM images of metallized microtubules after 1 min of metallization.

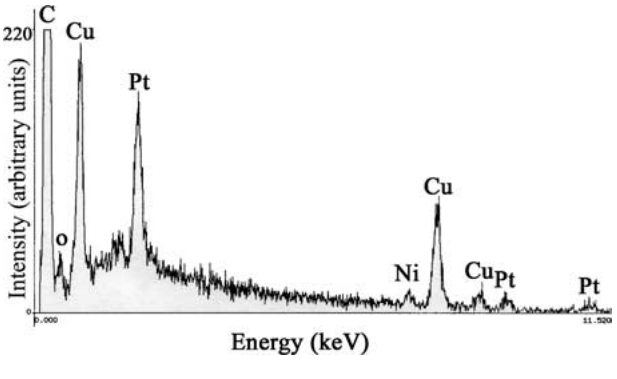

Figure 3 EDS spectrum for metallized microtubules after 1 min of electroless plating.

result from metallization of the big chunks or the clusters of MTs that survived the Pt-catalysis. SEM images of metallized MAP-stabilized MTs shows a continuous network of metallized microtubules after 1 min of electroless plating (Fig. 2). These metallized MTs are reasonably straight with diameter of about 30 to 35 nm and form a connected 3D network. The metal appears to have coated the MTs uniformly. A few metal clusters (diameter ∼5 to 15 nm) decorate the metallized MTs randomly.

The presence of platinum and nickel was confirmed using energy dispersive spectroscopy (EDS) (shown in Fig. 3). Apart from Ni and Pt, only copper, oxygen and carbon were identified. The copper and most of the carbon peaks result from the carbon-coated grid. The oxygen and a small fraction of the carbon peaks may come from the bio-molecular template. The element analysis indicates that the ratio of the number of Pt atoms to the number of Ni atoms is about 1.3:1. In addition to the catalysis of the protein surface with Pt, this ratio suggests that during the metallization stage, Pt was also deposited onto the MT surface.

In order to get more information about the interior of metallized MTs, they were characterized by TEM at 200 kV. Fig. 4 is the TEM micrograph of metallized MAP-stabilized MTs on a carbon substrate. This image

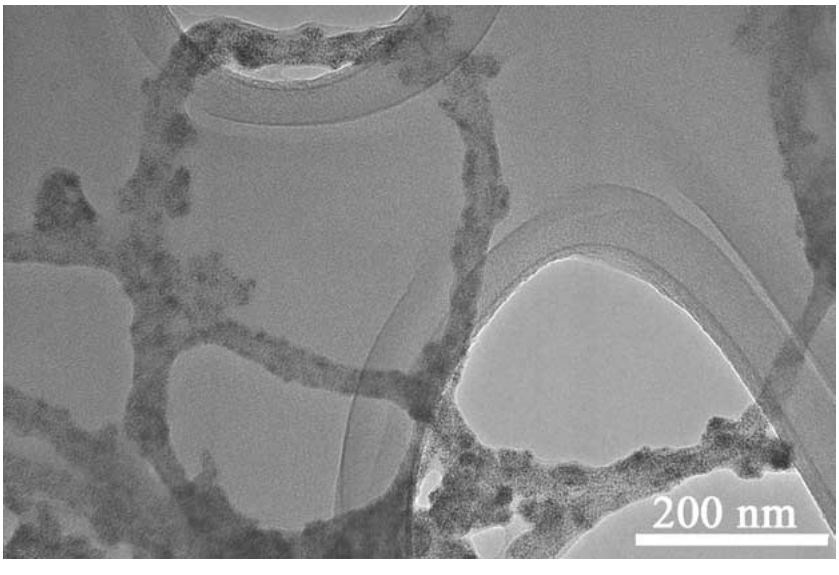

Figure 4 TEM micrograph of metallized MTs on carbon coated grid.

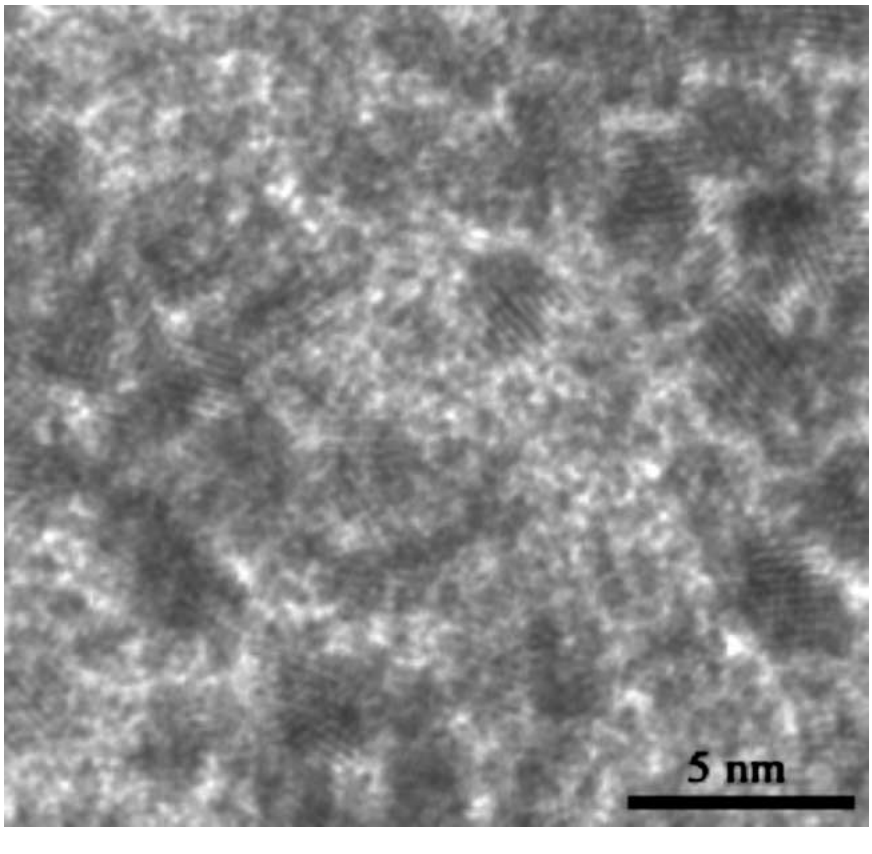

Figure 5 HRTEM micrograph of metallized MTs.

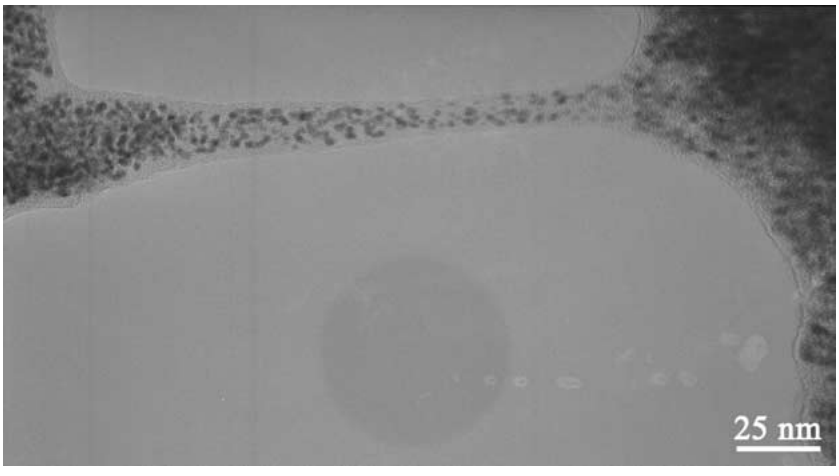

Figure 6 TEM micrograph of metallized MAPs bridge between MTs.

clearly shows that a network of nanowires is formed. The low contrast level of the nanowires means they are hollow metallized tubes, with thickness of about 30 to 35 nm. Fig. 4 suggests that regardless of whether Pt(II) could get into the lumen of MTs or not, there is little to no deposition of metal on its inner surface.

With higher resolution, some small black particles can be found embedded in the matrix of metallized tubes (Fig. 5). From this HRTEM image, more information on the metallized MTs surfaces is revealed. The black particles, which show lattice fringes, may be crystalline Pt clusters, which serve as a catalyst and initial nucleation center for subsequent electroless plating. The size of the Pt particles is measured to be about 3 nm by the scale of the lattice fringes. The randomly distributed and oriented Pt clusters are found all over the surface of MTs in low numbers. Most of MTs surface is covered with metals of amorphous phase, which is believed to be Ni.

Occasionally, metal bridges were observed between metallized microtubules (Fig. 6). These bridges have a diameter less than 15 nm, which is less than the MT template and too small to be seen in the SEM images. These bridges may come from MAPs protein bridges which cross-link microtubules. During the whole process of metallization, these proteins also could be catalyzed and metallized. With higher magnification, these bridges are shown to have a homogeneous microstructure of small dark Pt particles in amorphous metal matrix, similar to the metallized tubules.

5. Conclusions

In this paper, we have demonstrated the influence of MAPs on the stability of microtubules during the process of electroless plating with Ni and the final nanowire network. Our results show that MAPs are essential for MT stability during this process. In contrast to MTs made from pure tubulin MAP-stabilized MTs survived the Pt-catalysis step. Electroless plating of MAP-stabilized microtubules resulted in the formation of a continuous network of metallic nanowires. The metal coating consisted of small, crystalline Pt clusters embedded in an amorphous metal matrix composed of Ni distributed along the entire surface of the microtubules. More investigations should be done to reduce the amount of Pt in the metallized coating. Transmission electron microscopy detected very small, narrow metal bridges between larger nanowires. Both the metallized MTs and bridges are of the same microstructure, but different diameters, suggesting that these small diameter bridges may result from MAP complexes, not microtubules, and could be very important for interconnection of the nanowire network.

Acknowledgements

We would like to acknowledge financial support from the National Science Foundation, grant #0303863. This work was supported in part by a small research grant from the office of the Vice President for Research at the University of Arizona and the University of Arizona Foundation. We would like to acknowledge additional financial support from the College of Engineering and Mines and the department of Materials Science and Engineering at the University of Arizona. We thank Supapan Seraphin, Gary Chandler and Philip Anderson for assistance with HRTEM, TEM and SEM Characterization. We greatly appreciate the assistance with MT polymerization provided by Koen Visscher of the department of Physics and Helen YS Chen of the Biomedical Engineering Program at the University of Arizona.

References

1. N. C. SEEMAN and A. M. BELCHER, *PNAS* **99** (2002) 6451.
2. C. A. MIRKIN, *Mater. Res. Soc. Bull.* **25** (2000) 43.
3. A. P. ALIVISATOS, K. P. JOHNSSON, X. G. PENG, T. E. WILSON, C. J. LOWETH, M. B. BRUCHEZ and P. G. SCHULTZ, *Nature* **382** (1996) 609.
4. J. K. N. MIRBINDYO, B. D. RESIS, B. R. MARTIN, C. D. KEATING, M. J. NATAN and T. E. MALLOUK, *Adv. Mater.* **13** (2001) 249.
5. E. BRAUN, Y. EICHEN, U. SIVAN and G. BEN-YOSEPH, *Nature* **391** (1998) 775.
6. S. VAUTHEY, S. SANTOSO, H. GONG, N. WATSON and S. ZHANG, *PNAS* **99** (2002) 5355.
7. G. E. DOUBERLY, S. PAN, D. WALTERS and H. MATSUI, *J. Phys. Chem.* B **105** (2001) 7621.
8. H. MATSUI, P. PORRATA and G. E. DOUBERLY, *Nano Lett.* **1** (2001) 461.

9. G. M. CHOW, M. PAZIRANDEH, S. BARAL and J. R. CAMPBELL, *Nano-Struct. Mater.* **2** (1993) 495.
10. T. SCHEIBEL, R. PARTHASARATHY, G. SAWICKI, X. LIN, H. M. JAEGER and S. L. LINDQUIST, *Proc. Natl. Acad. Sci. USA* **100** (2003) 4527.
11. M. MERTIG, R. KIRSCH and W. POMPE, *Appl. Phys.* A **66** (1998) S723.
12. K. KINOSHITA, I. ARNAL, A. DESAI, D. N. DRECHSEL and A. A. HYMAN, *Science* **294** (2001) 1340.
13. S. BEHRENS, K. RAHN, N. HABICHT, K. J. BOHM, H. ROSNER, E. DINJUS and E. UNGER, *Adv. Mater.* **14**(22) (2002) 1621.
14. R. KIRSCH, M. MERTIG, W. POMPE, R. WAHL, G. SADOWSKI, K. J. BOHM and E. UNGER, *Thin Solid Films* **305** (1997) 248.
15. S. C. SCHUYLER and D. PELLMAN, *Cell.* **105**(4) (2001) 421.
16. M. J. SCHILSTRA, P. M. BAYLEY and S. R. MARTIN, *Biochem. J.* **227** (1991) 839.
17. L. A. AMOS and L. JAN, *Chem. Biol.* **6** (1999) 65.
18. I. ARNAL and R. H. WADE, *Curr. Biol.* **5** (1995) 900.
19. A. DESAI and T. J. MITCHISON, *Annu. Rev. Cell Dev. Biol.* **13** (1997) 83.
20. H. FELGNER, R. FRANK, J. BIERNAT, E. M. MANDELKOW, E. MANDELKOW, B. LUDIN, A. MATUS and M. SCHLIWA, *J. Cell. Biol.* **138** (1997) 1067.
21. E. HAMEL, A. A. DELCAMPO, M. LOWE and C. M. LIN, *J. Biol. Chem.* **256** (1981) 11887.
22. T. S. AHMADI, Z. L. WANG, T. C. GREEN, A. HENGLEIN and M. A. EL-SAYED, *Science* **272** (1997) 1924.
23. L. C. CIACCHI, P. WOLFGANG and D. V. ALESSANDRO, *J. Amer. Chem. Soc.* **123** (2001) 7371.

Received 18 August
and accepted 24 November 2003